JOURNAL OF AIRCRAFT
Vol. 47, No. 4, July–August 2010

Validation Studies for Aeroelastic Trim and Stability Analysis of Highly Flexible Aircraft

Zahra Sotoudeh* and Dewey H. Hodges†
Georgia Institute of Technology, Atlanta, Georgia 30332-0150
and
Chong-Seok Chang‡
Advanced Rotorcraft Technology, Inc., Mountain View, California 94043

DOI: 10.2514/1.46974

High-altitude, long-endurance (HALE) aircraft are highly flexible, requiring nonlinear aeroelastic analysis. NATASHA (Nonlinear Aeroelastic Trim and Stability of HALE Aircraft) is a computer program developed to analyze the aeroelastic behavior of HALE aircraft. The underlying formulation is based on the published geometrically exact, fully intrinsic beam equations. This paper presents a wide range of results from NATASHA, comparing them with well-known solutions of beam stability and vibration problems, experimental data, or results from well-established computer codes. Despite the simplicity of the underlying formulation, results obtained confirm the accuracy of the analysis and its suitability for conceptual and preliminary design of HALE aircraft.

Nomenclature

a	=	deformed beam aerodynamic frame of reference
B	=	deformed beam cross-sectional frame of reference
$\mathbf{B}_i$	=	unit vectors of deformed beam cross-sectional frame of reference ($i = 1, 2, 3$)
b	=	undeformed beam cross-sectional frame of reference
$\mathbf{b}_i$	=	unit vectors in undeformed beam cross-sectional frame of reference ($i = 1, 2, 3$)
c	=	chord
$c_{l\alpha}$	=	lift coefficient with respect to angle of attack α
$c_{m\beta}$	=	pitch moment coefficient with respect to flap deflection β
$c_{l\beta}$	=	lift coefficient with respect to flap deflection β
e	=	offset of aerodynamic center from the origin of frame of reference along $\mathbf{b}_2$
e_1	=	column matrix $\lfloor 1 \quad 0 \quad 0 \rfloor^T$
F	=	column matrix of internal force measures in $\mathbf{B}_i$ basis
f	=	column matrix of distributed applied force measures in $\mathbf{B}_i$ basis
H	=	column matrix of cross-sectional angular momentum measures in $\mathbf{B}_i$ basis
i	=	inertial frame of reference
$\mathbf{i}_i$	=	unit vectors for inertial frame of reference ($i = 1, 2, 3$)
I	=	cross-sectional inertia matrix
K	=	column matrix of deformed beam curvature and twist measures in $\mathbf{B}_i$ basis
k	=	column matrix of undeformed beam initial curvature and twist measures in $\mathbf{b}_i$ basis
M	=	column matrix of internal moment measures in $\mathbf{B}_i$ basis
m	=	column matrix of distributed applied moment measures in $\mathbf{B}_i$ basis
P	=	column matrix of cross-sectional linear momentum measures in $\mathbf{B}_i$ basis
r	=	column matrix of position vector measures in $\mathbf{b}_i$ basis
u	=	column matrix of displacement vector measures in $\mathbf{b}_i$ basis
V	=	column matrix of velocity measures in $\mathbf{B}_i$ basis
x_1	=	axial coordinate of beam
β	=	trailing-edge flap angle
γ	=	column matrix of 1-D generalized force strain measures
Δ	=	identity matrix
κ	=	column matrix of elastic twist and curvature measures (1-D generalized moment strain measures)
λ_0	=	induced-flow velocity
μ	=	mass per unit length
ξ	=	column matrix of center of mass offset from the frame of reference origin in $\mathbf{b}_i$ basis
ψ	=	column matrix of small incremental rotations
Ω	=	column matrix of cross-sectional angular velocity measures in $\mathbf{B}_i$ basis
$\dot{}$	=	partial derivative respect to time

Superscript

$'$	=	partial derivative with respect to x_1

I. Introduction

OVER the past decade, attention has turned to high-altitude, long-endurance (HALE) aircraft for a variety of applications. HALE aircraft typically have very flexible high-aspect-ratio wings. Therefore, wing deformation may be large during flight for this type of aircraft, and so linear theory generally predicts incorrect aeroelastic behavior. Accurate prediction of the aircraft response requires using nonlinear models for both structure and aerodynamics. Several published works by Patil et al. [1–3] treat various aspects of the aeroelasticity of high-aspect-ratio wings: in particular, showing the importance of including nonlinearities. To provide conceptual and preliminary design capability for highly flexible aircraft, development was initiated on at least two nonlinear analyses, one by Patil and Hodges [4] and the other by Shearer and Cesnik [5]. The present paper focuses on validation of the former, i.e., the computer program NATASHA (Nonlinear Aeroelastic Trim and Stability of HALE Aircraft). It is hoped that other researchers can use the results

Presented at the International Forum of Aeroelasticity and Structural Dynamics, Seattle, WA, 22–24 June 2009; received 1 September 2009; revision received 8 May 2010; accepted for publication 8 May 2010.

*Graduate Research Assistant, Daniel Guggenheim School of Aerospace Engineering; Zahra@gatech.edu. Student Member AIAA.
†Professor, Daniel Guggenheim School of Aerospace Engineering; Dhodges@gatech.edu. Fellow AIAA.
‡Aerospace Engineer; chong@flightlab.com. Member AIAA.

presented herein as benchmarks for their own codes. Finally, the present paper intends to illustrate the capabilities and versatility of the fully intrinsic formulation.

NATASHA is a nonlinear analysis based on applying the fully intrinsic beam formulation [6] along with 2-D aerodynamics and the finite state induced-flow model of Peters et al. [7] to analyze aeroelastic characteristics of flying wings [4]. The fully intrinsic beam equations are geometrically exact and have neither displacement nor rotation variables. They have no singularities associated with finite rotation variables and the maximum degree of nonlinearity is quadratic. Since the first version of NATASHA, its capability has been extended and improved. NATASHA can provide trim and stability analyses for flying wings as well as conventional wing–fuselage–tail configurations. Moreover, methodology has now been developed for statically indeterminate configurations, such as a joined-wing aircraft. NATASHA also has the capability of simulating a ground vibration test (GVT), providing the static equilibrium state as well as natural frequencies and mode shapes about that static equilibrium state. Note, however, that the GVT simulation and joined-wing analysis capability is not yet fully integrated into the most recent version of NATASHA, version 3.1. The gust response analysis of NATASHA is still undergoing validation. Published work on the theoretical developments can be found in [4,8–11].

Although this paper is mostly dedicated to validation of NATASHA, the governing equations and methodology are briefly reviewed in the second section. A wide range of results obtained from NATASHA are compared with those from well-known beam stability and vibration problems, published experimental data and results obtained from another computer code. For cases without available experimental results, NATASHA results are compared with those of RCAS (Rotorcraft Comprehensive Analysis System) [12]. RCAS is a well-validated, complex, general-purpose, comprehensive rotorcraft code with significant overhead, requiring of new users a significant investment of time. Since it is primarily a rotorcraft code, working with it requires some knowledge of rotorcraft, which is not necessary for analyses devoted to fixed-wing aircraft.

II. Fully Intrinsic Equations

A. Frames of Reference

The following frames of reference are used in NATASHA:

1) The inertial frame of reference is i. The unit vector $\mathbf{i}_3$ is in the opposite direction of gravity.

2) The undeformed beam frame of reference is b. The unit vector $\mathbf{b}_1$ is tangent to the beam reference line; $\mathbf{b}_2$ and $\mathbf{b}_3$ are unit vectors along the cross-sectional axes in which the cross-sectional stiffness and inertia matrices are calculated. The unit vector $\mathbf{b}_2$ points nominally toward the front of the airplane.

3) The deformed beam cross-sectional frame of reference is B.

4) The aerodynamic frame of reference is a. Aerodynamic lift and moment are defined in this frame; $\mathbf{a}_1 = \mathbf{b}_1$, $\mathbf{a}_2$ is parallel to the zero-lift line, and $\mathbf{a}_3 = \mathbf{a}_1 \times \mathbf{a}_2$ is perpendicular to it.

B. Governing Equations

The fully intrinsic equations can be written as six partial differential equations of motion, six kinematical partial differential equations, six algebraic structural constitutive equations and six algebraic inertial constitutive equations. In each case, because they are written in matrix form, they are shown as two matrix equations. The equations of motion are

$$F_B' + \tilde{K}_B F_B + f_B = \dot{P}_B + \tilde{\Omega}_B P_B$$
$$M_B' + \tilde{K}_B M_B + (\tilde{e}_1 + \tilde{\gamma}) F_B + m_B = \dot{H}_B + \tilde{\Omega}_B H_B + \tilde{V}_B P_B \quad (1)$$

where the generalized strains and velocities are related to stress resultants and moments by the structural constitutive equations

$$\begin{Bmatrix} \gamma \\ \kappa \end{Bmatrix} = \begin{bmatrix} R & S \\ S^T & T \end{bmatrix} \begin{Bmatrix} F_B \\ M_B \end{Bmatrix} \quad (2)$$

and the inertial constitutive equations:

$$\begin{Bmatrix} P_B \\ H_B \end{Bmatrix} = \begin{bmatrix} \mu\Delta & -\mu\tilde{\xi} \\ \mu\tilde{\xi} & I \end{bmatrix} \begin{Bmatrix} V_B \\ \Omega_B \end{Bmatrix} \quad (3)$$

Finally, the strain- and velocity-displacement equations were used to derive the intrinsic kinematical partial differential equations [6], which are given as

$$V_B' + \tilde{K}_B V_B + (\tilde{e}_1 + \tilde{\gamma})\Omega_B = \dot{\gamma} \qquad \Omega_B' + \tilde{K}_B \Omega_B = \dot{\kappa} \quad (4)$$

In this set of equations, F_B and M_B are column matrices of cross-sectional stress and moment resultant measures in the B frame, respectively; V_B and Ω_B are column matrices of cross-sectional frame velocity and angular velocity measures in the B frame, respectively; P_B and H_B are column matrices of cross-sectional linear and angular momentum measures in the B frame, respectively; R, S, and T are 3×3 partitions of the cross-sectional flexibility matrix; Δ is the 3×3 identity matrix; I is the 3×3 cross-sectional inertia matrix; ξ is $\lfloor\, 0 \quad \xi_2 \quad \xi_3 \,\rfloor^T$ with ξ_2 and ξ_3 the position coordinates of the cross-sectional mass center with respect to the reference line; μ is the mass per unit length; the tilde denotes the antisymmetric 3×3 matrix associated with the column matrix over which the tilde is placed; a dot denotes the partial derivative with respect to time; and prime denotes the partial derivative with respect to the coordinate along the beam axis, x_1. More details about these equations can be found in [13].

This is a complete set of first-order partial differential equations. To solve this complete set of equations, one may eliminate γ and κ using Eq. (2) and P_B and H_B using Eq. (3). Then 12 boundary conditions are needed, in terms of force F_B, moment M_B, velocity V_B, and angular velocity Ω_B.

If needed, position and orientation can be calculated as a postprocessing operation by integrating

$$r_i' = C^{ib} e_1 \qquad (r_i + u_i)' = C^{iB}(e_1 + \gamma) \quad (5)$$

and

$$(C^{bi})' = -\tilde{k} C^{bi} \qquad (C^{Bi})' = -(\tilde{k} + \tilde{\kappa}) C^{Bi} \quad (6)$$

C. Solution Procedure in NATASHA

The dependence of the equations on x_1 is removed from the partial differential equations by use of spatial central differencing. Next, the resulting nonlinear ordinary differential equations are linearized about a static equilibrium state. The equilibrium state is governed by nonlinear algebraic equations, which NATASHA solves in obtaining the steady-state trim solution. For statically determinate structures (such as flying-wing or conventional aircraft configurations) this system of nonlinear algebraic equations is solved using the Newton–Raphson procedure. However, for statically indeterminate structures (such as a joined-wing aircraft configuration), the fully intrinsic equations are not sufficient. To get around this NATASHA uses an incremental version of the equations governing the static equilibrium [11]. The incremental method solves sequential sets of linear equations in which the loading is increased in small steps. The fully intrinsic equations, when linearized about the resulting trim state, lead to a standard eigenvalue problem. This part of the solution procedure is the same for statically determinate or indeterminate structures. It should be noted that NATASHA also has the capability to do time-marching solutions and uses the fully intrinsic equations to determine them.

III. Results From Validation Studies

Three types of validation are considered in this paper. First, NATASHA is exercised to obtain results for a variety of classical problems, including problems in vibration, buckling and aeroelasticity. Second, validation against a very limited set of experimental data is included. Finally, results from NATASHA are compared with those obtained from a conventional aircraft configuration modeled using the well-established computer program RCAS [12].

A. Validation for Classical Problems

Table 1 shows general structural properties used for the beam stability and vibration examples; SI units are used for all properties and results. Table 2 shows the results from NATASHA for a variety of such problems, including Euler buckling of a cantilevered beam (see page 88 of [14]); lateral-torsional buckling of a cantilevered beam (see page 265 of [15]); flutter load for the Beck problem, a cantilevered beam under compressive axial follower force (see page 306 of [15]); lateral-torsional flutter load for a lateral follower force at the tip of a cantilevered beam [16]; flutter thrust for a free–free beam under compressive axial follower force, close approximations in the literature being [17,18]; and aeroelastic divergence and reversal for a cantilevered wing [19]. For reversal and divergence calculations, the aerodynamic model is a steady-flow, strip theory [19].

Note that control reversal may be defined differently, depending on the application. For example, a control reversal speed for a cantilevered wing may be defined as the speed at which the total lift changes sign. This is equivalent to the speed at which the shear force at the root of the beam vanishes if one ignores all applied forces other than lift. Thus, one finds the speed at which the total lift [19] vanishes, viz.,

$$\int_0^L cq[c_{l_\beta}\beta + c_{l_\alpha}\theta(x_1)]\,\mathrm{d}x_1 = 0 \tag{7}$$

where q is the dynamic pressure. Alternatively, one may also define reversal as occurring when the out-of-plane bending moment at the root of the wing changes sign, so that

$$\int_0^L cqx_1[c_{l_\beta}\beta + c_{l_\alpha}\theta(x_1)]\,\mathrm{d}x_1 = 0 \tag{8}$$

Moment and shear force are direct output of the fully intrinsic equations; therefore, finding reversal speed by studying the moment and shear force at the root is more direct via the fully intrinsic equations than using a displacement approach.

In addition, flutter results were obtained for the Goland wing, properties of which are available in [20]. For aeroelastic flutter analysis, NATASHA uses a strip theory aerodynamic model with the 2-D induced-flow model of Peters et al. [4,7] plus the apparent mass terms. Flutter analysis was performed for the Goland wing [20] using NATASHA with 20 elements. NATASHA results are $V=$ 451 ft/ sec and flutter frequency of 70.1 rad/ sec, whereas exact results are $V = 450$ ft/ sec with flutter frequency equal to 70.7 rad/ sec. Note that results from the mixed formulation of [21] are $V = 445$ ft/ sec and flutter frequency of 70.2 rad/ sec.

Table 1 Beam properties for classical validations (SI units)

Length	16
Torsional stiffness	10^4
Out-of-plane bending stiffness	2×10^4
In-plane bending stiffness	4×10^6
Mass per unit length	0.75
Mass polar moment of inertia per unit length	0.1
Chord c	1
Offset of aerodynamic center from elastic axis e	0.25
Lift-curve slope $c_{l\alpha}$	2π
Lift-curve derivative with respect to flap angle $c_{l\beta}$	3.7
Moment-curve derivative with respect to flap angle $c_{m\beta}$	−0.5

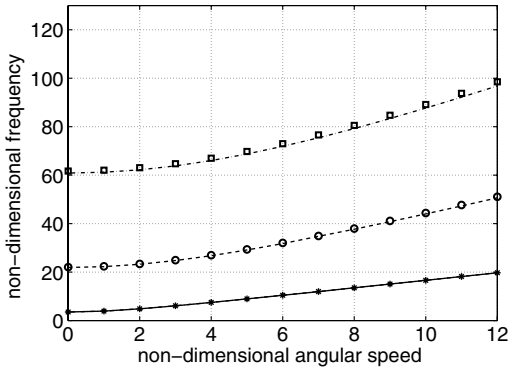

Fig. 1 Natural frequencies $\omega\sqrt{mL^4/EI}$ of a clamped–free rotating beam; lines are NATASHA's results and symbols are from [22].

Natural frequencies of both nonrotating and rotating beams in a vacuum can be calculated as accurately as one pleases. For example, Fig. 1 shows the first three out-of-plane (i.e., flap) bending natural frequencies of a clamped–free rotating beam. These results for nondimensional frequencies $\omega\sqrt{mL^4/EI}$ are essentially the same as those of [22].

B. Validation Against Experimental Results

1 Validation Against Princeton Beam Experiments

The Princeton beam experiments [23] have been used for decades as a benchmark for validations of nonlinear beam theories. NATASHA has been used to regenerate all the results presented in [24]. Both the mixed formulation [24] and the fully intrinsic equations used in NATASHA are geometrically exact. As expected, all the present results are essentially the same as those presented in [24] excepting very small numerical differences caused by differing solution methods. Therefore, only a small subset of these results are presented here. Figures 2 and 3 show the out-of-plane and in-plane tip deflections, respectively, versus setting angle for different applied tip forces. Figure 4 shows results for the lowest bending frequency from the Princeton beam experiments and from NATASHA versus the applied force P for a zero setting angle ($\theta = 0$). The value of P at which the frequency is equal to zero is the lateral-torsional buckling load for this beam, as corrected for prebuckling deflection [25]. The Princeton beam results show that the fully intrinsic equations of NATASHA are capable of accurately capturing geometrically nonlinear effects.

Generally, NATASHA needs more elements than displacement-based programs such as DYMORE [26]. However, NATASHA involves only the simplest possible elements and nonlinearities no higher than second degree. Despite being based on simple and inexpensive elements, the NATASHA formulation is capable of capturing nonlinearities with accuracy comparable to that of a geometrically exact mixed formulation.

Table 2 Results obtained for classical validations (SI units)

Problem	Exact solution	NATASHA results	No. of elements
Euler buckling	192.766	192.843	32
Lateral-torsional buckling	222.577	222.769	32
Beck flutter load	1566.48	1575.04	32
Beck flutter frequency	7.027	7.058	32
Lateral-torsional flutter thrust	334.57	335.06	32
Free-free beam flutter thrust	8568.8	8654.7	40
Divergence	37.1539	37.2737	8
Reversal (zero root shear)	24.902	24.917	16
Reversal (zero root bending moment)	23.29	23.31	16

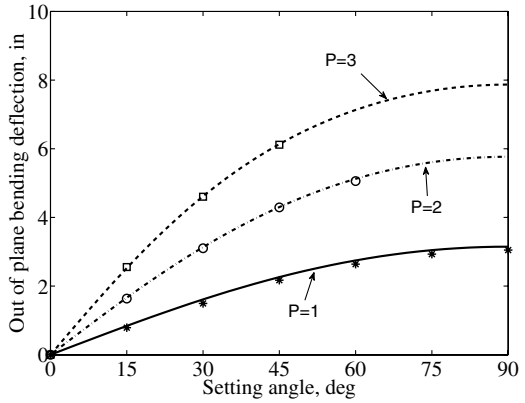

Fig. 2 NATASHA results (lines) vs Princeton beam experiments (symbols); *P* is the applied force at the beam tip.

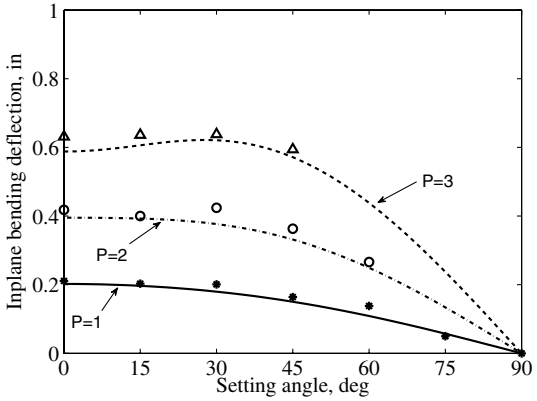

Fig. 3 NATASHA results (lines) vs Princeton beam experiments (symbols); *P* is the applied force at the beam tip.

2 Validation of NATASHA for Joined-Wing Aircraft

The incremental method as applied to the fully intrinsic equations is validated by comparing its results with those from the Newton–Raphson solution of the mixed-formulation equations [27] and with experimental data [28]. Figure 5 shows top and front views of the test structure. The details of structural properties and loading can be found in [27,28].

Figure 6 shows the joint deflection versus tip load. Results obtained from the incremental method are in excellent agreement with those from the mixed formulation. Neither formulation perfectly matches the experimental data after a certain point because of yielding of the joint [27]. Figure 7 shows the tip deflection of the same structure under varying tip load for the incremental method, the

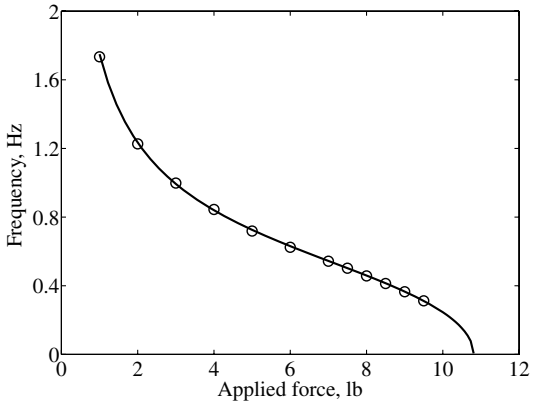

Fig. 4 NATASHA results (lines) vs Princeton beam experiments (symbols); the setting angle is zero.

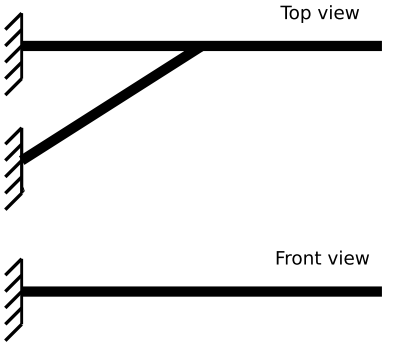

Fig. 5 Joined-wing configuration.

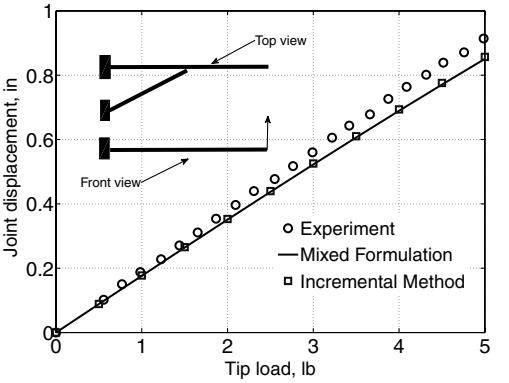

Fig. 6 Joint deflection

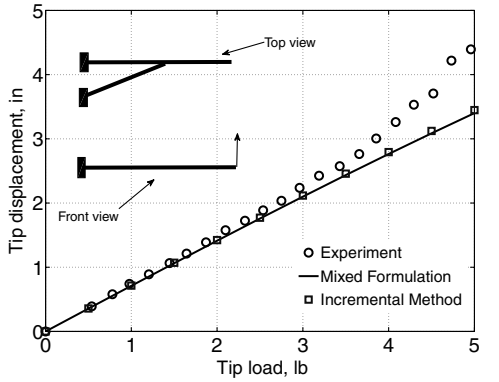

Fig. 7 Tip deflection.

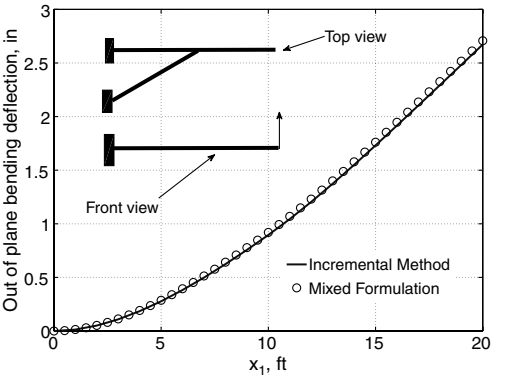

Fig. 8 Out-of-plane bending deflection.

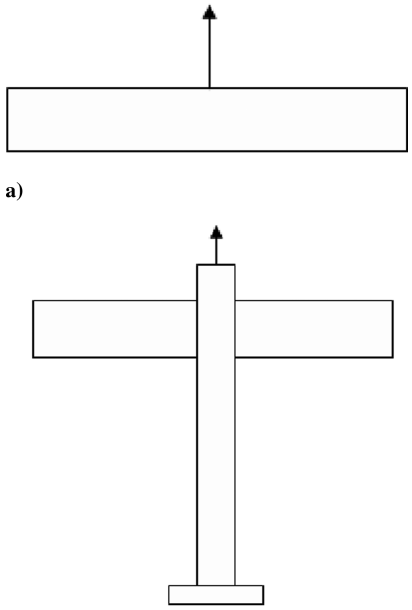

Fig. 9 Sample configurations to validate NATASHA.

mixed formulation, and experimental results. Figure 8 shows the out-of-plane bending deflection of the main wing of the same structure under a constant load distribution [27]. The mixed formulation and incremental method are in excellent agreement with each other and are both close to the experimental results.

C. Validation of NATASHA Using RCAS

In this study RCAS results are used as a benchmark to validate NATASHA. RCAS [12] is a comprehensive rotorcraft analysis code, developed by the Army Aeroflightdynamics Directorate at NASA Ames Research Center and Advanced Rotorcraft Technology, Inc., to provide an interdisciplinary, comprehensive analysis tool for rotorcraft analysis and design. RCAS uses a finite element approach, and it has several available aerodynamic models from which to choose.

1. Description of Models

Figure 9 shows the two models that are used in this study. Figure 9a is a flying-wing configuration. The trim variables are the magnitude of thrust, the angle of attack and a spanwise constant flap deflection. Figure 9b shows a conventional aircraft configuration with fuselage, wing, and horizontal tail. Structural properties for the flying-wing configuration are given in Table 3, and those for the conventional aircraft are taken from [10]; the payload for both models is simulated by a point mass at midspan.

There are important differences between the two models, the two solution procedures and the two codes:

1) RCAS was developed primarily for rotorcraft analysis and NATASHA was developed primarily for HALE aircraft analysis. In NATASHA, flap deflection and thrust magnitude are free variables used to determine the trim state. Since RCAS was designed to be a rotorcraft code, however, the rotor angular speed is a specified parameter and therefore not available as a free variable to determine the trim state. In results presented herein the trim state in RCAS is computed using a specified angular speed derived from the NATASHA trim state.

2) There are also differences between the aerodynamic models in NATASHA and RCAS. With respect to flap deflections, NATASHA uses linear relations between the aerodynamic loads and flap defections in terms of lift and moment coefficients. On the other hand, RCAS uses the Theordorsen airfoil/elevon theory, which evaluates lift and moment deficiency functions from elevon deflection. First, the deficiency coefficients in RCAS are chosen arbitrarily to make the angle of attack without payload case matches closely to the result of NATASHA. Then the angle of attack is fixed for other payload cases to see if at least the results are consistent through the whole simulation.

3) There are also some small differences in the structural models. The body and tail in conventional aircraft configurations are modeled as very stiff beams in NATASHA, but they are rigid bodies in RCAS.

4) Finally, some differences are inevitable due to limitations of NATASHA's control system model. These and other differences may lead to disparities between the results obtained from NATASHA and those obtained from RCAS, especially for the conventional aircraft configuration. In spite of all these differences between the models and solution procedures, all results from NATASHA show the right trends, and NATASHA's relative errors only become significant for quantities that are very small in magnitude.

Table 3 Beam properties for RCAS validations of flying-wing configuration (Fig. 9a)

Elastic axis (reference line)	25% chord
Torsional stiffness	0.4×10^6 lb-ft^2
Out-of-plane bending stiffness	2.5×10^6 lb-ft^2
In-plane bending stiffness	30×10^6 lb-ft^2
Mass per unit length	0.1863 slug/ft
Center of gravity	25% chord
Sectional centroidal mass moments of inertia:	
About the x_1 axis (torsional)	30 slug-ft
About the x_2 axis	5 slug-ft
About the x_3 axis	25 slug-ft

2. Results from NATASHA and RCAS

In this section, results for trim condition and natural frequencies for two different configurations from NATASHA and RCAS are presented in Figs. 10–19. Although NATASHA's results agree well

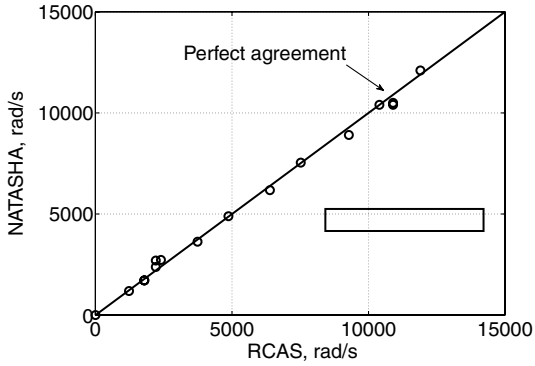

Fig. 10 Frequencies of flying wing for NATASHA vs RCAS. Both RCAS and NATASHA results are in rad/s.

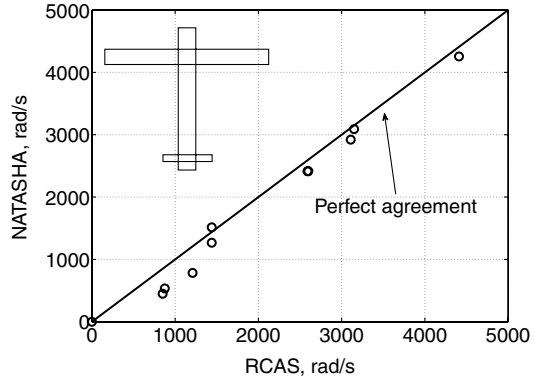

Fig. 11 Frequencies of conventional aircraft for NATASHA vs RCAS. Both RCAS and NATASHA results are in rad/s.

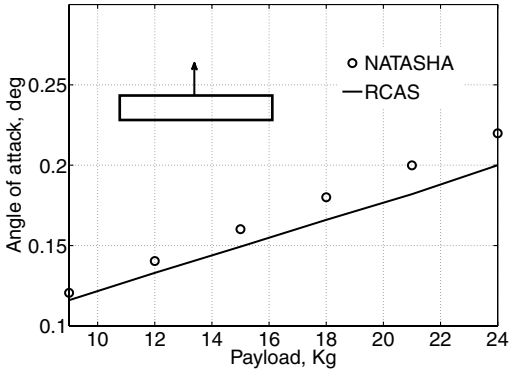

Fig. 12 Angle of attack vs midspan mass.

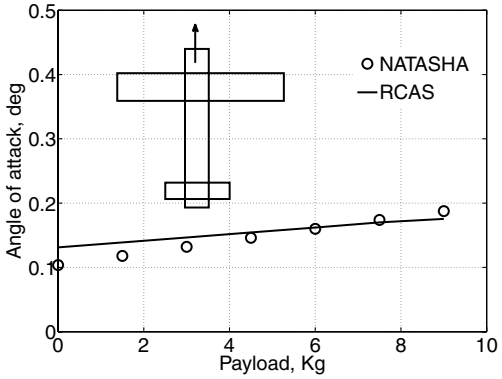

Fig. 13 Angle of attack vs midspan mass.

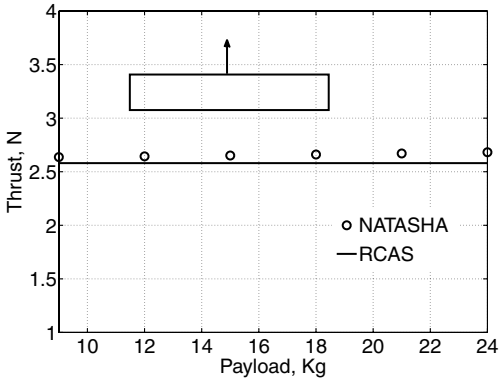

Fig. 14 Thrust vs midspan mass.

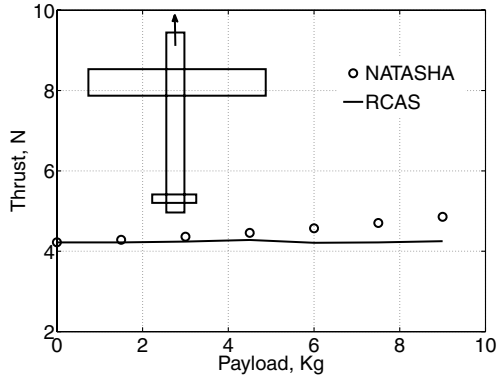

Fig. 15 Thrust vs midspan mass.

with those of RCAS, the results are not identical because of differences between the two codes and their respective models.

Figures 10 and 11 show, respectively, the first several natural frequencies in a vacuum for a flying-wing configuration and for a conventional configuration from NATASHA and RCAS. The agreement between the codes is excellent for the flying-wing configuration, but the agreement for the conventional configuration is not as good. Although the actual reasons are unknown to the authors, this discrepancy is quite possibly because RCAS models the body and tail as rigid bodies, whereas NATASHA models them as beams, albeit with relatively large bending and torsional stiffnesses.

This discrepancy in natural frequencies for the conventional configuration does not have any deleterious effect on the aeroelastic results, which show NATASHA and RCAS in very good agreement. Figures 12 and 13 show the change of angle of attack at trim versus the mass of the payload at midspan for both flying-wing and conventional aircraft configurations. Figures 14 and 15 show the change of thrust for steady, level flight of flying-wing and conventional aircraft configurations versus the mass of the payload at midspan. Results agree for the flying wing somewhat better than they do for the conventional aircraft configuration, but in both cases the trends are captured accurately by NATASHA.

The next set of results is for the distributions of shear force and bending moment for both flying-wing and conventional aircraft configurations. Figures 16 and 17 show the distributions of shear force and moment along the wing span in a flying wing, expressed in the deformed beam reference frame at each node. Note that for this test case the midspan mass is 9 kg, and the axial force F_1 and twisting moment M_1 are both zero. Results from NATASHA and RCAS are essentially identical for this case. Figures 18 and 19 show the distributions of shear force and bending moment for conventional aircraft with zero midspan mass. These results agree well, though there are some relatively small discrepancies. These are most likely caused by differences in the way trim variables are set and in the aerodynamic models used for elevator in the tail.

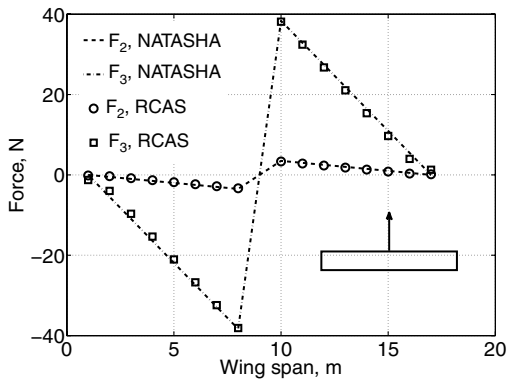

Fig. 16 Shear force distribution along wing span.

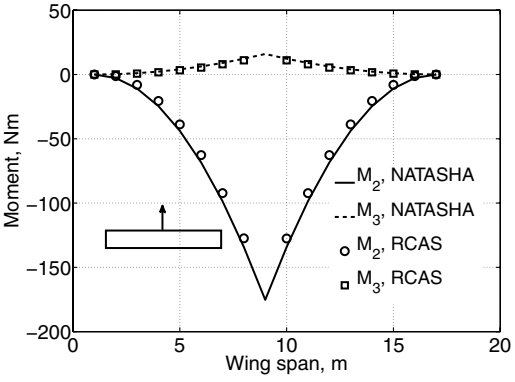

Fig. 17 Bending moment distribution along wing span.

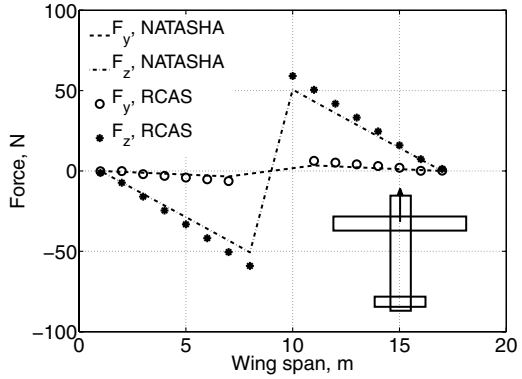

Fig. 18 Shear force distribution along wing span.

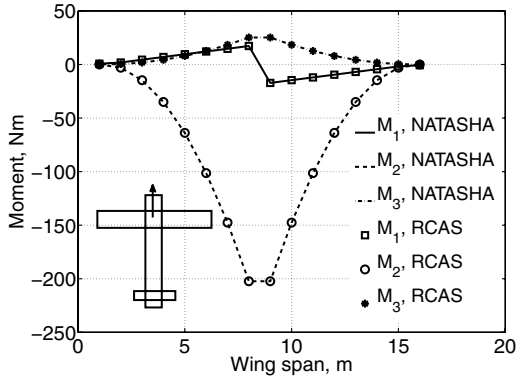

Fig. 19 Bending moment distribution along wing span.

Overall, the results show the trends for predicted behavior of the system versus any of the parameters are essentially the same whether predicted by NATASHA or by RCAS. Therefore, NATASHA can be used with confidence for conceptual and preliminary design of HALE aircraft.

IV. Conclusions

NATASHA can perform a nonlinear aeroelastic analysis of the trim and stability of HALE aircraft, along with visualization. Because it is important for any analysis tool to be extensively validated, this paper contains many validation results for nonlinear structural analysis, structural dynamics, and aeroelasticity. In particular, the accuracy of results obtained from NATASHA, as compared to those from beam stability problems and experimental data, is excellent. Moreover, results obtained from NATASHA agree quite well with those of more sophisticated analysis tools such as RCAS. It is concluded that NATASHA can be a useful tool, providing acceptable accuracy for conceptual and preliminary design of HALE aircraft. It is recommended that additional validation studies be conducted by comparison of results with those of [5].

References

[1] Patil, M. J., Hodges, D. H., and Cesnik, C. E. S., "Nonlinear Aeroelasticity and Flight Dynamics of High-Altitude, Long-Endurance Aircraft," *Journal of Aircraft*, Vol. 38, No. 1, Jan.–Feb. 2001, pp. 88–94. doi:10.2514/2.2738

[2] Patil, M. J., Hodges, D. H., and Cesnik, C. E. S., "Limit Cycle Oscillations in High-Aspect-Ratio Wings," *Journal of Fluids and Structures*, Vol. 15, No. 1, Jan. 2001, pp. 107–132. doi:10.1006/jfls.2000.0329

[3] Patil, M. J., and Hodges, D. H., "On the Importance of Aerodynamic and Structural Geometrical Nonlinearities in Aeroelastic Behavior of High-Aspect-Ratio Wings," *Journal of Fluids and Structures*, Vol. 19, No. 7, Aug. 2004, pp. 905–915. doi:10.1016/j.jfluidstructs.2004.04.012

[4] Patil, M. J., and Hodges, D. H., "Flight Dynamics of Highly Flexible Flying Wings," *Journal of Aircraft*, Vol. 43, No. 6, 2006, pp. 1790–1799. doi:10.2514/1.17640

[5] Shearer, C. M., and Cesnik, C. E. S., "Nonlinear Flight Dynamics of Very Flexible Aircraft," *Journal of Aircraft*, Vol. 44, No. 5, 2007, pp. 1528–1545. doi:10.2514/1.27606

[6] Hodges, D. H., "Geometrically Exact, Intrinsic Theory for Dynamics of Curved and Twisted Anisotropic Beams," *AIAA Journal*, Vol. 41, No. 6, June 2003, pp. 1131–1137. doi:10.2514/2.2054

[7] Peters, D. A., Karunamoorthy, S., and Cao, W.-M., "Finite State Induced Flow Models; Part I: Two-Dimensional Thin Airfoil," *Journal of Aircraft*, Vol. 32, No. 2, Mar.–Apr. 1995, pp. 313–322. doi:10.2514/3.46718

[8] Patil, M. J., and Taylor, D. J., "Gust Response of Highly Flexible Aircraft," 47th Structures, Structural Dynamics, and Materials Conference, Newport, RI, AIAA, Paper 2006-1638, May 2006.

[9] Chang, C.-S., and Hodges, D. H., "Parametric Studies on Ground Vibration Test Modeling for Highly Flexible Aircraft," *Journal of Aircraft*, Vol. 44, No. 6, Nov.–Dec. 2007, pp. 2049–2059. doi:10.2514/1.30733

[10] Chang, C.-S., Hodges, D. H., and Patil, M. J., "Flight Dynamics of Highly Flexible Aircraft," *Journal of Aircraft*, Vol. 45, No. 2, Mar.–Apr. 2008, pp. 538–545. doi:10.2514/1.30890

[11] Sotoudeh, Z., and Hodges, D. H., "Nonlinear Aeroelastic Analysis of Joined-Wing Aircraft with Intrinsic Equations," 50th Structures, Structural Dynamics, and Materials Conference, Palm Springs, CA, AIAA Paper 2009-2464, May 2009.

[12] Saberi, H. A., Khoshlahjeh, M., Ormiston, R. A., and Rutkowski, M. J., "RCAS Overview and Application to Advanced Rotorcraft Problems," *4th Decennial Specialists' Conference on Aeromechanics*, AHS International, Alexandria, VA, Jan. 2004.

[13] Hodges, D. H., *Nonlinear Composite Beam Theory*, AIAA, Reston, VA, 2006.

[14] Timoshenko, S. P., and Gere, J. M., *Theory of Elastic Stability*, 2nd ed., McGraw–Hill, New York, 1961.

[15] Simitses, G. J., and Hodges, D. H., *Fundamentals of Structural Stability*, Elsevier, Boston, 2006.

[16] Hodges, D. H., "Lateral-Torsional Flutter of a Deep Cantilever Loaded by a Lateral Follower Force at the Tip," *Journal of Sound and Vibration*, Vol. 247, No. 1, Oct. 2001, pp. 175–183. doi:10.1006/jsvi.2001.3624

[17] Beal, T. R., "Dynamic Stability of a Flexible Missile under Constant and Pulsating Thrusts," *AIAA Journal*, Vol. 3, No. 3, March 1965, pp. 486–494. doi:10.2514/3.2891

[18] Sundararamaiah, V., and Johns, D. J., "Comment on 'On the Stability of a Free-Free Beam Under Axial Thrust Subjected to Directional Control'," *Journal of Sound and Vibration*, Vol. 48, No. 4, 1976, pp. 571–573. doi:10.1016/0022-460X(76)90561-7

[19] Hodges, D. H., and Pierce, G. A., *Introduction to Structural Dynamics and Aeroelasticity*, Cambridge Univ. Press, Cambridge, England, U.K., 2002.

[20] Goland, M., and Luke, Y. L., "The Flutter of a Uniform Wing with Tip Weights," *Journal of Applied Mechanics*, Vol. 15, No. 1, 1948, pp. 13–20.

[21] Patil, M. J., Hodges, D. H., and Cesnik, C. E. S., "Nonlinear Aeroelastic Analysis of Complete Aircraft in Subsonic Flow," *Journal of Aircraft*, Vol. 37, No. 5, Sept.–Oct. 2000, pp. 753–760. doi:10.2514/2.2685

[22] Hodges, D. H., and Rutkowski, M. J., "Free-Vibration Analysis of Rotating Beams by a Variable-Order Finite Element Method," *AIAA Journal*, Vol. 19, No. 11, Nov. 1981, pp. 1459–1466. doi:10.2514/3.60082

[23] Dowell, E. H., Traybar, J., and Hodges, D. H., "An Experimental-Theoretical Correlation Study of Non-Linear Bending and Torsion Deformations of a Cantilever Beam," *Journal of Sound and Vibration*, Vol. 50, No. 4, 1977, pp. 533–544. doi:10.1016/0022-460X(77)90501-6

[24] Hodges, D. H., and Patil, M. J., "Correlation of Geometrically Exact Beam Theory with the Princeton Data," *Journal of the American Helicopter Society*, Vol. 49, No. 3, July 2004, pp. 357–360. doi:10.4050/JAHS.49.357

[25] Hodges, D. H., and Peters, D. A., "On the Lateral Buckling of Uniform Slender Cantilever Beams," *International Journal of Solids and*

Structures, Vol. 11, No. 12, Dec. 1975, pp. 1269–1280. doi:10.1016/0020-7683(75)90056-6

[26] Bauchau, O. A., "DYMORE User's Manual," 2007, http://ae.gatech.edu/people/obauchau/Dwnld/dymore30/DymoreManual.pdf [retrieved 2010].

[27] Patil, M. J., "Nonlinear Aeroelastic Analysis of Joined-Wing Aircraft," 44th Structures, Structural Dynamics and Materials Conference, Norfolk, VA, AIAA Paper 2003-1487, April 2003.

[28] Dreibelbis, B., and Barth, J., "Structural Analysis of Joint Wings," *Proceedings of Regional Student Conference*, AIAA, Reston, VA, April 2003.